J. Membrane Biol. 131, 237–243 (1993)

The Journal of
Membrane Biology

The Cyclic Nucleotide-Activated Conductance in Olfactory Cilia: Effects of Cytoplasmic Mg^{2+} and Ca^{2+}

Steven J. Kleene
Department of Anatomy and Cell Biology, University of Cincinnati, Cincinnati, Ohio 45267-0521

Summary. Olfactory receptor neurons depolarize in response to odorants. This depolarization is mediated by an increase in intracellular cyclic AMP, which directly gates channels in the membranes of the neuronal cilia. Previous evidence suggests that a Ca^{2+} influx during the odorant response may ultimately play a role in terminating the response. One way Ca^{2+} inside the cell could terminate the odorant response would be to directly inhibit the cAMP-gated channels. In this report the effects of cytoplasmic Ca^{2+} and Mg^{2+} on the cAMP-activated current were measured in single olfactory cilia. Near the neuronal resting potential, cytoplasmic Ca^{2+} and Mg^{2+} only slightly reduced the cAMP-activated current. Even at high levels (1.0 mM Ca^{2+} or 5.0 mM Mg^{2+}), the average inhibition was only around 20%. It is therefore unlikely that an influx of divalent cations terminates the odorant response by a direct effect on the cAMP-gated channels.

Key Words olfaction · receptor neuron · cilia · cyclic-nucleotide-gated channel · calcium · magnesium

Introduction

Olfactory receptor neurons depolarize transiently in response to odorous stimulation. There is now clear evidence for at least one mechanism of depolarization. Many odorants activate an olfactory adenylate cyclase in vitro [19, 22, 25, 26]. The product of adenylate cyclase, cAMP, directly gates transmembrane channels in the olfactory cilia [16, 21]. The cAMP-activated conductance has a reversal potential near 0 mV, and its activation depolarizes the neuron [8, 15, 20, 28, 31].

Why the neuronal depolarization is transient remains to be established. In isolated cilia, odorants stimulate production of cAMP, but the cAMP level subsequently falls in a manner that depends on protein kinase A [2]. In intact neurons, an inward current induced by odorants is long-lasting unless extracellular Ca^{2+} is present [17, 35]. It thus seems likely that Ca^{2+} may carry some of the inward current [23, 24] and indirectly lead to termination of the odorant response. A simple mechanism for Ca^{2+}-dependent termination of the response has been proposed [35]. In this model, Ca^{2+} flowing in during the odorant response directly inhibits the cAMP-gated channels. Single cAMP-gated channels of the neuronal dendrite were shown to be strongly inhibited by cytoplasmic Ca^{2+} near physiological levels [35]. However, the function of cAMP-gated channels in the soma and dendrite remains obscure.

Although it is well documented that the primary sites of odorant transduction are in the olfactory cilia [9, 14, 18], there have been few characterizations of the ciliary cAMP-activated conductance [16, 21]. By patch-clamp recording from single olfactory cilia [12], I have determined the effects of cytoplasmic Ca^{2+} and Mg^{2+} on the macroscopic ciliary current activated by cAMP. In the cilia, Ca^{2+} and Mg^{2+} cause only slight inhibition of the cAMP-activated current under physiological conditions. Such inhibition is unlikely to be of functional significance during the odorant response.

Materials and Methods

Ciliary Patch

Single olfactory receptor neurons were isolated from the northern grass frog (*Rana pipiens*) and the land phase tiger salamander (*Ambystoma tigrinum*). For each experiment, one cilium of a neuron was sucked into a patch pipette until a high-resistance seal formed near the base of the cilium. By raising the pipette briefly into air, the cilium was excised from the cell. The cilium remained sealed inside the recording micropipette with the cytoplasmic face of the membrane exposed to the bath. The pipette containing the cilium could be quickly transferred through the air to various pseudointracellular baths without rupturing the seal. Although the current-voltage relation usually became stable within 2 sec after transfer to a new bath, 20 sec was routinely allowed before recording the relation. Complete details of the ciliary patch procedure have been presented elsewhere [12].

Table 1. Compositions of solutions (mM)

Solutions	NaCl	KCl	$MeSO_3H$	$CaCl_2$	Calcium gluconate	$MgCl_2$	Magnesium gluconate	EDTA	NaOH	KOH
Extracellular										
Standard	115	3	—	1	—	2	—	—	2	—
Ca^{2+}, Mg^{2+}-free	115	3	—	—	—	—	—	1	4	—
Cl^--free	—	—	118	—	1	—	2	—	117	3
Ca^{2+}, Mg^{2+}, Cl^--free	—	—	118	—	—	—	—	1	119	3
Pseudointracellular										
Standard (low Ca^{2+})	5	110	—	0.8	—	0–5.0			—	9
Mg^{2+}, Cl^--free	—	—	115	—	0.7–3.0	—			5	119

Abbreviation used: $MeSO_3H$, methanesulfonic acid. All solutions contained 5 mM HEPES and were adjusted to pH 7.2. All pseudointracellular solutions also contained 2 mM BAPTA. In the standard pseudointracellular solution $[Ca^{2+}]_{free}$ was 0.1 μM. Concentrations listed for $MgCl_2$ in the standard pseudointracellular solution and for calcium gluconate in the Mg^{2+}, Cl^--free pseudointracellular solution are the ranges used in the dose-response studies. In the Cl^--free solutions, most of the NaOH or KOH added served to neutralize the $MeSO_3H$, producing a methanesulfonate salt (115 or 118 mM) and water.

Solutions

Solutions used are defined in Table 1. Extracellular solutions were used to bathe intact cells and to fill the recording pipettes. The cell suspension was stored in standard extracellular solution. For patch formation, a single cell was transferred to a bath containing an extracellular solution. This was the same solution used to fill the recording pipette, with one difference. While the solution in the pipette contained 1 mM EDTA, the bath solution instead contained 2 mM $MgCl_2$ and 1 mM $CaCl_2$. It was nearly impossible to form high-resistance seals without divalent cations in the bath. The small amount of Ca^{2+} and Mg^{2+} sucked into the pipette during the patch procedure was quickly chelated by EDTA in the pipette. After seal formation, chelation was detectable as a gradual increase in cAMP-activated current at negative potentials, as the blocking effect of the external divalent cations [6, 21, 36] was relieved. This process was usually complete within 1 min. For Fig. 1, patch formation was done in the standard extracellular solution, while the pipette contained Ca^{2+}, Mg^{2+}-free solution. For Figs. 2 and 3, patch formation was done in the Cl^--free extracellular solution, while the pipette contained Ca^{2+}, Mg^{2+}, Cl^--free solution.

After a cilium was excised from a neuron, the pipette was lowered into a pseudointracellular solution, which then bathed the cytoplasmic face of the ciliary membrane. The pipette containing the cilium was quickly transferred through the air to various pseudointracellular baths without rupturing the seal. Complete details have been presented elsewhere [12].

All pseudointracellular solutions contained at least 0.1 μM free Ca^{2+}, which helped to stabilize the seal. $[Ca^{2+}]_{free}$ was buffered with BAPTA [1,2-bis(*o*-aminophenoxy)ethane-*N*,*N*,*N'*,*N'*-tetraacetic acid], a highly Ca^{2+}-specific chelator [32]. $[Ca^{2+}]_{free}$ in the pseudointracellular solutions was calculated using apparent association constants K'_{Ca} determined in triplicate by the method of Bers [1]. The K'_{Ca} values were 6.62×10^6 M^{-1} in 115 mM KCl and 5.01×10^6 M^{-1} in 115 mM potassium methanesulfonate, both containing 5 mM HEPES and adjusted to pH 7.2. Gluconate$^-$ was avoided as a Cl^- substitute since gluconate$^-$ itself binds Ca^{2+} [4]. BAPTA was included in all pseudointracellular solutions for consistency, even though its buffer capacity was exceeded in some cases. Poorest control was in the solution designed to have 10 μM free Ca^{2+}. A 2% error in $[Ca^{2+}]_{total}$ would cause $[Ca^{2+}]_{free}$ to be 5 or 26 μM, depending on the direction of the error. The calcium gluconate stock solution was calibrated with a Ca^{2+}-specific electrode (Orion 932000) by comparison with a standard 0.1 M $CaCl_2$ solution (Orion 922006). The BAPTA stock solution was calibrated as described by Bers [1]. Binding of Mg^{2+} by BAPTA in the pseudointracellular solutions was negligible [13, 32].

Electrical Recording

Both the recording pipette and chamber were coupled to a List L/M-EPC7 patch-clamp amplifier by Ag/AgCl electrodes. All recordings were done under voltage clamp at room temperature (25°C). Current was adjusted to zero with the open pipette in the well in which the patching procedure was done. The solutions in the bath and the tip of the pipette were identical at this stage, except for divalent cations as described above. This difference caused a liquid junction potential at the pipette tip of <1 mV, which was corrected for as described by Hagiwara and Ohmori [10]. After excision of a cilium, the pipette was transferred through a series of wells containing modified pseudointracellular solutions. Each of these wells was connected by a salt bridge to a common reference bath. A correction was applied for the liquid junction potential between each pseudointracellular bath and its salt bridge [10].

When studying the effect of intracellular Ca^{2+} on the cAMP-activated conductance, it was first necessary to eliminate a ciliary Cl^- current that is activated by cytoplasmic Ca^{2+} [13]. This was done by replacing Cl^- on both sides of the membrane with methanesulfonate$^-$. Since both Ag/AgCl electrodes required Cl^- to function stably and reversibly, salt bridges were used to connect the electrodes to the Cl^--free solutions. The salt bridge between the pipette and reference baths was made of polyethylene tubing. Both the reference bath and this salt bridge contained standard extracellular solution; the salt bridge also included 5% (*w/v*) agarose. A second salt bridge was made within the patch pipette. This bridge connected the tip of the patch pipette and the recording electrode, a Ag/AgCl wire within the pipette. The bottom 1 cm of the pipette, which bathed the ciliary membrane, was filled with the Ca^{2+}, Mg^{2+}, Cl^--free extracellular solution plus 0.07% (*w/v*) agarose (Sigma Type I). On top of this was layered the standard (Cl^--containing) extracellular solution, which covered the recording wire electrode. This intrapipette salt bridge has been described in detail elsewhere [11].

Voltage ramps (−100 to +100 mV, 0.2 mV/msec) were generated by pCLAMP software (Axon Instruments). Current-voltage records were acquired at a sampling rate of 500 Hz. In all records, an upward deflection represents increasing positive current from the bath into the pipette. Potentials are reported as bath (cytoplasmic) potential relative to pipette potential. To estimate a reversal potential, a 12-mV region surrounding the apparent reversal potential was fit to a straight line. The voltage-intercept of this line was taken as the reversal potential. Current values at a given voltage were calculated by averaging a 10-mV region surrounding the given voltage. Results of repeated experiments are reported as mean ± SEM. The Student's *t*-test was used for statistical comparisons. Reagents were purchased from Sigma.

cAMP-Activated Current

For each cilium, a current-voltage plot was first acquired in the appropriate pseudointracellular solution with no cAMP added. Subsequently, current-voltage relations were measured in the presence of 100 μM cAMP and various levels of divalent cations as described. In all figures, the cAMP-free control has been subtracted, so that the current-voltage relations shown represent only the current activated by 100 μM cytoplasmic cAMP. The control measured in the absence of cAMP depended slightly on $[Ca^{2+}]_{free}$, but this difference was small compared to the cAMP-activated current. Expressed as slope conductance between −70 and −30 mV, the controls subtracted averaged 6 ± 1% (Fig. 1, $n = 6$); 7 ± 1% (Fig. 2, $n = 14$); and 6 ± 1% (Fig. 3, $n = 8$) of the total conductance measured in the presence of 100 μM cAMP and low divalent cations. Cyclic-AMP phosphodiesterase activity was detectable in the cilia (*not shown*). However, addition of the phosphodiesterase inhibitor 3-isobutyl-1-methylxanthine did not alter the current activated by the saturating levels of cAMP used here.

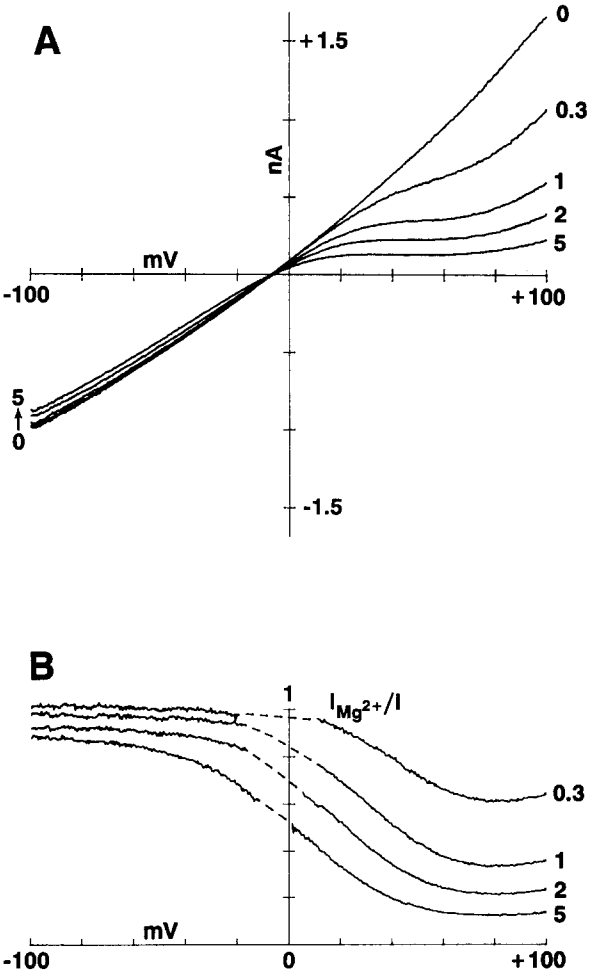

Fig. 1. Inhibition of the cyclic nucleotide-activated conductance in frog olfactory cilia by cytoplasmic Mg^{2+}. (*A*) The current-voltage relationship of the ciliary membrane was measured in each of five baths. Baths consisted of the standard pseudointracellular solution plus 100 μM cAMP and Mg^{2+} from 0 to 5 mM as indicated. The recording pipette contained Ca^{2+}, Mg^{2+}-free extracellular solution. Current measured in the absence of cAMP was subtracted as described in Materials and Methods, so that only the cAMP-activated current is shown. Each current-voltage plot is the average of determinations in six cilia. (*B*) Replot of Fig. 1*A* to show the voltage dependence of inhibition by cytoplasmic Mg^{2+}. For each current-voltage curve in Fig. 1*A*, the current at each voltage was normalized to the value at the same voltage measured in the absence of cytoplasmic Mg^{2+}. Since meaningful ratios were unobtainable near the reversal potential, a simple connection has been drawn between the two halves of each curve (*dashed lines*).

Results

To test the effects of cytoplasmic Mg^{2+} and Ca^{2+} on the ciliary cAMP-activated conductance, recordings were made from single cilia excised from frog olfactory receptor neurons [12]. One cilium of a cell was sucked inside a patch pipette. A high-resistance seal was made between the base of a cilium and the tip of the pipette, and the pipette containing the cilium was detached from the cell. The cilium remained inside the pipette with the cytoplasmic face of its membrane exposed to the bath [12]. EDTA was included in the pipette to prevent external divalent cations from blocking the cAMP-gated channels [6, 21, 36].

Effects of Cytoplasmic Magnesium

Figure 1 shows the current-voltage properties of the ciliary cAMP-activated conductance as cytoplasmic (bath) Mg^{2+} was varied. Bath solutions included 0.1 μM free Ca^{2+} to stabilize the membrane-pipette seal. In the absence of cytoplasmic Mg^{2+}, the cAMP-activated conductance was nearly linear, with a slope averaging 13.1 ± 1.6 nS (measured between −90 and 90 mV, range 7.2 to 17.5 nS, $n = 6$) and a reversal potential of −6.7 ± 0.9 mV (range −9.5 to −2.5 mV, $n = 6$). Cytoplasmic Mg^{2+} caused only a

slight inhibition of the cAMP-activated current at negative potentials, but the outward current at positive potentials was greatly decreased (Fig. 1*A*). Inhibition was complete within 1 sec after the cilium was transferred to the Mg^{2+}-containing bath, and the inhibition was fully reversed within 1 sec on return to a Mg^{2+}-free bath. The complex shape of the current-voltage relation in the presence of cytoplasmic Mg^{2+} was unaltered by reducing the speed of the voltage ramp tenfold or by reversing the direction of the ramp. In Fig. 1*B*, the data in Fig. 1*A* have been replotted to more clearly show the strong voltage dependence of inhibition by cytoplasmic Mg^{2+}. Each current-voltage relation in the presence of cytoplasmic Mg^{2+} was divided by that in the absence of Mg^{2+} to show the fraction of cAMP-activated current remaining at each voltage.

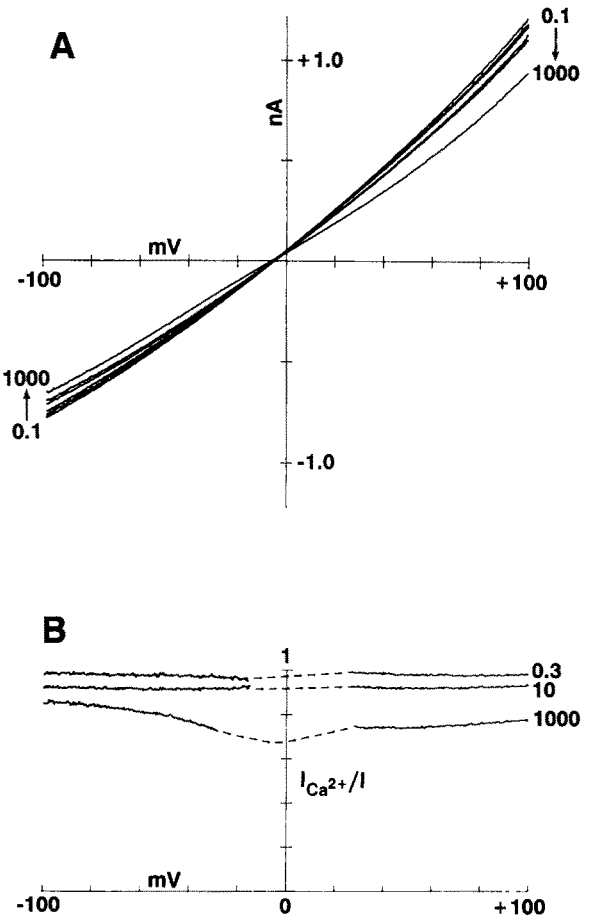

Fig. 2. Inhibition of the cyclic nucleotide-activated conductance in frog olfactory cilia by cytoplasmic Ca^{2+}. (*A*) The current-voltage relationship of the ciliary membrane was measured in each of six baths. Baths consisted of the Mg^{2+}, Cl^--free pseudointracellular solution plus 100 μM cAMP and free Ca^{2+} of 0.1, 0.3, 1, 10, 100, or 1000 μM. The effects of increasing free Ca^{2+} were monotonic as indicated by the *arrows*. The recording pipette contained Ca^{2+}, Mg^{2+}, Cl^--free extracellular solution. Current measured in the absence of cAMP was subtracted as described in Materials and Methods, so that only the cAMP-activated current is shown. Each current-voltage plot is the average of determinations in 14 cilia. (*B*) Replot of Fig. 2*A* to show the voltage dependence of inhibition by cytoplasmic Ca^{2+}. For each current-voltage curve in Fig. 2*A*, the current at each voltage was normalized to the value at the same voltage measured in the lowest free Ca^{2+} (0.1 μM). For clarity only three of the curves are shown.

Effects of Cytoplasmic Calcium

To measure the effects of cytoplasmic Ca^{2+} on the cAMP-activated current, it was first necessary to eliminate current through a ciliary Ca^{2+}-activated Cl^- conductance [13]. To do this, Cl^- on both sides of the ciliary membrane was replaced by methanesulfonate$^-$. Under this condition, elevating cytoplasmic Ca^{2+} from 0.1 μM to 1 mM caused an average conductance increase of just 0.3 ± 0.1 nS (measured between −70 and −30 mV, n = 14), compared to 3.6 nS in Cl^--containing solutions [13].

With 0.1 μM cytoplasmic Ca^{2+} in the bath, the conductance activated by cAMP had a slope averaging 9.9 ± 0.8 nS (measured between −90 and 90 mV, range 4.9 to 15.5 nS, n = 14) and a reversal potential of −4.8 ± 1.0 mV (range −10.2 to +2.9 mV, n = 14). Ionic conditions for the maximal currents in Figs. 1 and 2 were identical except for replacement of Cl^- in the experiments of Fig. 2. There was no significant difference between the maximal currents in the two cases ($P > 0.05$). Even at very high concentrations, cytoplasmic Ca^{2+} had little effect on the ciliary cAMP-activated current (Fig. 2). In about half of the cilia tested, the small inhibition by cytoplasmic Ca^{2+} was fully reversed upon return to a bath containing 0.1 μM free Ca^{2+}. In others, the effect was only partly reversible. Inhibition by Ca^{2+} at −50 mV never exceeded 35% in any single experiment. Inhibition of the cAMP-activated current by cytoplasmic Ca^{2+} showed little voltage dependence (Fig. 2*B*).

If the EDTA in the pipette was replaced by 2 mM Mg^{2+} and 1 mM Ca^{2+}, the inward cAMP-activated current was greatly reduced due to external block by divalent cations [6, 21, 36]. The remaining current was inhibited somewhat more effectively by cytoplasmic Ca^{2+} than when EDTA was in the pipette (*not shown*). At −50 mV, 1 μM Ca^{2+} in the bath inhibited the cAMP-activated current by 19.8 ± 5.2% (n = 5), while 100 μM Ca^{2+} caused an inhibition of 31.0 ± 8.4% (n = 5).

The small effect of cytoplasmic Ca^{2+} on the ciliary cAMP-activated current was surprising. In the tiger salamander (*Ambystoma tigrinum*), cAMP-gated channels from the dendrites of olfactory recep-

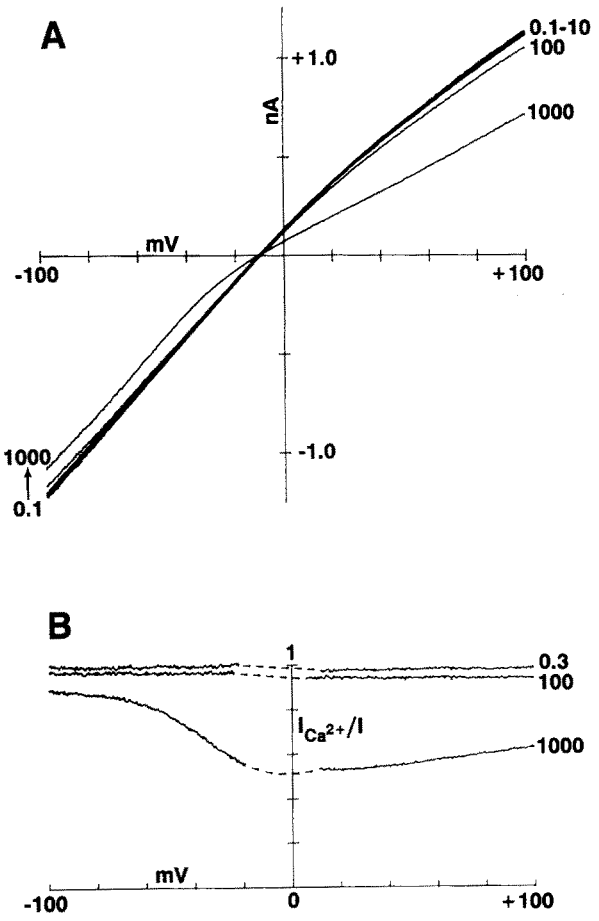

Fig. 3. Inhibition of the cyclic nucleotide-activated conductance in salamander olfactory cilia by cytoplasmic Ca^{2+}. Procedures were identical to those described for Fig. 2. Each current-voltage plot is the average of determinations in eight cilia. For clarity only three of the curves are shown in part (*B*).

tor neurons were strongly affected by cytoplasmic Ca^{2+}. In particular, increasing free Ca^{2+} from 0.1 to 3 μM reduced the single-channel open probability from 0.6 to 0.09 [35]. However, the macroscopic cAMP-activated current in frog cilia never showed such a strong dependence on cytoplasmic Ca^{2+} (Fig. 2). In an attempt to resolve these two sets of results, I measured the effects of cytoplasmic Ca^{2+} on the cAMP-activated current in olfactory cilia from tiger salamanders (Fig. 3). Preliminary results (*not shown*) indicated that the salamander cilia, like those of the frog, have a Ca^{2+}-activated Cl^- conductance, so again Cl^- on both sides of the ciliary membrane was replaced by methanesulfonate$^-$. Only at 1 mM Ca^{2+} was a significant inhibition of the ciliary cAMP-activated current seen. With 0.1 μM cytoplasmic Ca^{2+}, the cAMP-activated conductance had a slope averaging 12.2 ± 1.5 nS (measured between −90 and 90 mV, range 5.3 to 19.4 nS, n = 8) and a reversal potential of −9.5 ± 0.8 mV (range −14.2 to −7.0 mV, n = 8). The inhibition caused by 1 mM Ca^{2+} was more pronounced at depolarized potentials (Fig. 3*B*).

Table 2 provides a summary of the effects of cytoplasmic Mg^{2+} and Ca^{2+} on the ciliary cAMP-activated current.

Discussion

The effects of cytoplasmic Mg^{2+} and Ca^{2+} on the macroscopic cAMP-activated current in olfactory cilia were determined. Both divalent cations were found to reduce the current. Cytoplasmic Mg^{2+} was especially effective, eliminating most of the current at positive membrane potentials (Fig. 1). Near resting potential, however, both divalent cations were very weak inhibitors, even when elevated beyond their physiological concentration ranges (Table 2). The slight inhibition seen showed little voltage dependence over the physiological range of potentials, so the level of inhibition should not change as the cell depolarizes.

Suzuki has reported similar effects of cytoplasmic divalent cations on cAMP-gated channels from the somata of bullfrog olfactory receptor neurons. At +60 mV, 1 mM Mg^{2+} completely blocked channel activity, while Ca^{2+} had a weaker effect [29]. At negative potentials, a combination of 10 μM Ca^{2+} and 1.25 mM Mg^{2+} failed to block current [30].

The results reported here conflict with a single-channel study of cAMP-gated channels from salamander olfactory dendrites [35]. In that study, physiological levels of intracellular free Ca^{2+} greatly reduced the open probability of the single channels at −60 mV. The open probability was decreased by about 40% with 1 μM Ca^{2+} and by 85% with 3 μM Ca^{2+}. In contrast, I found that inhibition of the cAMP-activated current in salamander olfactory cilia never exceeded 10% with 1 μM cytoplasmic Ca^{2+} and never exceeded 32% even when 1 mM Ca^{2+} was added (Table 2). The reason for this discrepancy is not clear. A difference between the cytoplasmic solutions used (KCl here and NaCl in the single channel study [35]) should be of little consequence. In both studies, the inward current carrier at negative potentials was undoubtedly Na^+. It is conceivable that the free Ca^{2+} concentrations reported here were actually reduced inside the cilium by a ciliary buffering or sequestering mechanism. There may also exist more than one type of cAMP-gated channel in a given species, or perhaps the membrane environments of the cilia and dendrite are different enough to result in markedly different channel properties. In any case, it has become apparent that sin-

Table 2. Inhibition of ciliary cAMP-activated current by cytoplasmic Mg^{2+} and Ca^{2+} at −50 mV

	% inhibition (mean ± SEM)	Range	*a*
Frog			
0 mM Mg^{2+}	(0)	—	6
0.3 mM Mg^{2+}	0.3 ± 0.4	−1.0 to 1.6	6
1.0 mM Mg^{2+}	4.0 ± 1.4	−1.9 to 7.0	6
2.0 mM Mg^{2+}	10.5 ± 2.2	3.3 to 15.6	6
5.0 mM Mg^{2+}	18.0 ± 3.0	9.0 to 24.4	6
0.1 μM Ca^{2+}	(0)	—	14
0.3 μM Ca^{2+}	2.4 ± 1.1	−4.8 to 7.6	14
1.0 μM Ca^{2+}	5.2 ± 1.6	−6.3 to 14.7	14
10 μM Ca^{2+}	8.8 ± 1.9	−1.4 to 20.7	14
100 μM Ca^{2+}	10.9 ± 2.3	0.2 to 25.3	14
1.0 mM Ca^{2+}	20.5 ± 2.8	2.0 to 35.1	14
Salamander			
0.1 μM Ca^{2+}	(0)	—	8
0.3 μM Ca^{2+}	0.3 ± 1.3	−3.9 to 7.3	8
1.0 μM Ca^{2+}	2.6 ± 1.5	−3.9 to 9.5	8
10 μM Ca^{2+}	2.5 ± 1.4	−4.1 to 8.7	8
100 μM Ca^{2+}	3.6 ± 2.7	−6.8 to 15.6	8
1.0 mM Ca^{2+}	22.8 ± 2.2	12.4 to 31.7	8

Values shown are the % reduction in cAMP-activated current measured at −50 mV compared to controls (0 mM Mg^{2+} or 0.1 μM Ca^{2+}). Current at −50 mV was determined by averaging all points on the current-voltage relation between −55 and −45 mV. Where the range includes a negative value, the divalent cation increased the current at −50 mV in that experiment. The lowest concentrations of divalent cations that produced significant inhibition ($P < 0.05$) were 1.0 mM Mg^{2+} and 1.0 μM Ca^{2+} in frog cilia and 1 mM Ca^{2+} in salamander cilia. Absolute values for the control currents were 505 ± 62 pA (frog, 0 mM Mg^{2+}); 406 ± 33 pA (frog, 0.1 μM Ca^{2+}); and 559 ± 67 pA (salamander, 0.1 μM Ca^{2+}).

gle channels of the dendrite are not always accurate predictors of the macroscopic current in the cilia.

A cGMP-activated current functions in vertebrate phototransduction. The effects of divalent cations on that current are similar to the effects reported here. Cytoplasmic Ca^{2+} has little effect on the cGMP-activated current under physiological conditions [5, 7, 27, 33, 34]. In membrane patches from rod outer segments of the toad, 1.6 mM cytoplasmic Ca^{2+} caused only a small inhibition of the macroscopic current at positive potentials (*see* Fig. 5 of ref. 33). However, 1.6 mM Mg^{2+} greatly reduced the cGMP-activated current at positive potentials [33]. In those experiments cGMP-activated current at negative potentials was largely blocked by external divalent cations. In patches from rods of the tiger salamander, Colamartino et al. [5] also reported inhibition by cytoplasmic divalent cations. The voltage dependence of inhibition was similar to that reported here for the ciliary current (Figs. 1*B*, 2*B*, 3*B*). In that study, the effect of cytoplasmic Ca^{2+} in the rod was somewhat stronger than that measured here in the olfactory cilia. In the rod membrane, 1 mM Ca^{2+} inhibited the cGMP-activated current by about 50% at −50 mV. In olfactory cilia from the same species, 1 mM Ca^{2+} reduced the cAMP-activated current by just 23% at −50 mV (Table 2; Fig. 3).

There is good evidence that Ca^{2+} enters the neuron during the odorant response [23, 24] and that this influx indirectly leads to termination of the response [17, 35]. One possible mechanism for this would be a direct inhibition of the cAMP-gated channels by Ca^{2+} accumulating within the cell [35]. The results presented here make this explanation unlikely; cytoplasmic Ca^{2+} has little ability to block the ciliary channels under physiological conditions. Other mechanisms have been suggested for Ca^{2+}-mediated termination of the odorant response. Calcium, together with calmodulin, activates a phosphodiesterase in rat olfactory cilia [3]. Thus, a Ca^{2+} influx could increase hydrolysis of cAMP and indirectly lead to closing of the cAMP-gated channels [8]. In the frog, Ca^{2+} activates a ciliary Cl^- conductance which also could modify the odorant response [13]. These mechanisms remain plausible.

I am grateful to Stuart Firestein, Robert Gesteland, and Raymund Pun for critical reviews of the manuscript. This work was supported by National Institutes of Health grants PO1 DC00347 and R55 DC00926.

References

1. Bers, D.M. 1982. A simple method for the accurate determination of free [Ca] in Ca-EGTA solutions. *Am. J. Physiol.* **242:**C404–408
2. Boekhoff, I., Breer, H. 1992. Termination of second messenger signaling in olfaction. *Proc. Natl. Acad. Sci. USA* **89:**471–474
3. Borisy, F.F., Ronnett, G.V., Cunningham, A.M., Juilfs, D., Beavo, J., Snyder, S.H. 1992. Calcium/calmodulin-activated phosphodiesterase expressed in olfactory receptor neurons. *J. Neurosci.* **12:**915–923
4. Christofferson, G.R.J., Skibsted, L.H. 1975. Calcium ion activity in physiological salt solutions: influence of anions substituted for chloride. *Comp. Biochem. Physiol.* **52A:** 317–322
5. Colamartino, G., Menini, A., Torre, V. 1991. Blockage and permeation of divalent cations through the cyclic GMP-activated channel from tiger salamander retinal rods. *J. Physiol.* **440:**189–206
6. Dhallan, R.S., Yau, K.-W., Schrader, K.A., Reed, R.R. 1990. Primary structure and functional expression of a cyclic nucleotide-activated channel from olfactory neurons. *Nature* **347:**184–187
7. Fesenko, E.E., Kolesnikov, S.S., Lyubarsky, A.L. 1986. Direct action of cGMP on the conductance of retinal rod plasma membrane. *Biochim. Biophys. Acta* **856:**661–671
8. Firestein, S., Darrow, B., Shepherd, G.M. 1991. Activation of the sensory current in salamander olfactory receptor neurons depends on a G protein-mediated cAMP messenger system. *Neuron* **6:**825–835
9. Firestein, S., Shepherd, G.M., Werblin, F. 1990. Time course of the membrane current underlying sensory transduction in salamander olfactory receptor neurones. *J. Physiol.* **430:**135–158
10. Hagiwara, S., Ohmori, H. 1982. Studies of calcium channels in rat clonal pituitary cells with patch electrode voltage clamp. *J. Physiol.* **331:**231–252
11. Kleene, S.J. 1993. A simple intrapipette salt bridge. *J. Neurosci. Methods* **46:**11–16
12. Kleene, S.J., Gesteland, R.C. 1991. Transmembrane currents in frog olfactory cilia. *J. Membrane Biol.* **120:**75–81
13. Kleene, S.J., Gesteland, R.C. 1991. Calcium-activated chloride conductance in frog olfactory cilia. *J. Neurosci.* **11:**3624–3629
14. Kurahashi, T. 1990. Activation by odorants of cation-selective conductance in the olfactory receptor cell isolated from the newt. *J. Physiol.* **419:**177–192
15. Kurahashi, T. 1990. The response induced by intracellular cyclic AMP in isolated olfactory receptor cells of the newt. *J. Physiol.* **430:**355–371
16. Kurahashi, T., Kaneko, A. 1991. High density cAMP-gated channels at the ciliary membrane in the olfactory receptor cell. *NeuroReport* **2:**5–8
17. Kurahashi, T., Shibuya, T. 1990. Ca^{2+}-dependent adaptive properties in the solitary olfactory receptor cell of the newt. *Brain Res.* **515:**261–268
18. Lowe, G., Gold, G.H. 1991. The spatial distributions of odorant sensitivity and odorant-induced currents in salamander olfactory receptor cells. *J. Physiol.* **442:**147–168
19. Lowe, G., Nakamura, T., Gold, G.H. 1989. Adenylate cyclase mediates olfactory transduction for a wide variety of odorants. *Proc. Natl. Acad. Sci. USA* **86:**5641–5645
20. Miyamoto, T., Restrepo, D., Cragoe, E.J., Jr., Teeter, J.H. 1992. IP_3- and cAMP-induced responses in isolated olfactory receptor neurons from the channel catfish. *J. Membrane Biol.* **127:**173–183
21. Nakamura, T., Gold, G.H. 1987. A cyclic nucleotide-gated conductance in olfactory receptor cilia. *Nature* **325:**442–444
22. Pace, U., Hanski, E., Salomon, Y., Lancet, D. 1985. Odorant-sensitive adenylate cyclase may mediate olfactory reception. *Nature* **316:**255–258
23. Restrepo, D., Miyamoto, T., Bryant, B.P., Teeter, J.H. 1990. Odor stimuli trigger influx of calcium into olfactory neurons of the channel catfish. *Science* **249:**1166–1168
24. Sato, T., Hirono, J., Tonoike, M., Takebayashi, M. 1991. Two types of increases in free Ca^{2+} evoked by odor in isolated frog olfactory receptor neurons. *NeuroReport* **2:**229–232
25. Shirley, S.G., Robinson, C.J., Dickinson, K., Aujla, R., Dodd, G.H. 1986. Olfactory adenylate cyclase of the rat. *Biochem. J.* **240:**605–607
26. Sklar, P.B., Anholt, R.R.H., Snyder, S.H. 1986. The odorant-sensitive adenylate cyclase of olfactory receptor cells. *J. Biol. Chem.* **261:**15538–15543
27. Stern, J.H., Kaupp, U.B., MacLeish, P.R. 1986. Control of the light-regulated current in rod photoreceptors by cyclic GMP, calcium, and *l-cis*-diltiazem. *Proc. Natl. Acad. Sci. USA* **83:**1163–1167
28. Suzuki, N. 1989. Voltage- and cyclic nucleotide-gated currents in isolated olfactory receptor cells. *In:* Chemical Senses, Vol. 1, Receptor Events and Transduction in Taste and Olfaction. J.G. Brand, J.H. Teeter, R.H. Cagan, M.R. Kare, editors. pp. 469–493. Marcel Dekker, New York
29. Suzuki, N. 1990. Single cyclic nucleotide-activated ion channel activity in olfactory receptor cell soma membrane. *Neurosci. Res.* **Suppl. 12:**S113–S126
30. Suzuki, N. 1991. Voltage-dependent block by divalent cations of cyclic nucleotide-activated channel activity and olfactory receptor cell adaptation. *Chem. Senses* **16:**206
31. Trotier, D., Rosin, J.-F., MacLeod, P. 1989. Channel activities in in vivo and isolated olfactory receptor cells. *In:* Chemical Senses, Vol. 1, Receptor Events and Transduction in Taste and Olfaction. J.G. Brand, J.H. Teeter, R.H. Cagan, M.R. Kare, editors. pp. 427–448. Marcel Dekker, New York
32. Tsien, R. 1980. New calcium indicators and buffers with high selectivity against magnesium and protons: design, synthesis, and properties of prototype structures. *Biochemistry* **19:**2396–2404
33. Yau, K.-W., Baylor, D.A. 1989. Cyclic GMP-activated conductance of retinal photoreceptor cells. *Annu. Rev. Neurosci.* **12:**289–327
34. Zimmerman, A.L., Baylor, D.A. 1992. Cation interactions within the cyclic GMP-activated channel of retinal rods from the tiger salamander. *J. Physiol.* **449:**759–783
35. Zufall, F., Shepherd, G.M., Firestein, S. 1991. Inhibition of the olfactory cyclic nucleotide gated ion channel by intracellular calcium. *Proc. R. Soc. Lond. B* **246:**225–230
36. Zufall, F., Shepherd, G.M., Firestein, S. 1992. Block of the olfactory, cyclic nucleotide gated ion channel by extracellular calcium and magnesium ions. *Biophys. J.* **61:**A283

Received 10 June 1992; revised 18 August 1992